Title: Movement kinematics dynamically modulates the rolandic ~20-Hz rhythm during goal-directed executed and observed *hand actions*.

Abbreviated title: Modulation of mu rhythm by movement kinematics

Authors: Marty B.[1], Bourguignon M.[1,2,3,4], Jousmäki V.[1,3], Wens V.[1,5], Goldman S.[1,5] and De Tiège X.[1,5]

[1]Laboratoire de Cartographie fonctionnelle du Cerveau, UNI – ULB Neuroscience Institute, Université libre de Bruxelles (ULB), Brussels, Belgium.

[2]Laboratoire Cognition Langage et Développement, UNI – ULB Neuroscience Institute, Université libre de Bruxelles (ULB), Brussels, Belgium.

[3]Department of Neuroscience and Biomedical Engineering and Aalto NeuroImaging, Aalto University School of Science, PO Box 12200, 00076 AALTO, Espoo, Finland.

[4]BCBL, Basque Center on Cognition, Brain and Language, 20009 San Sebastian, Spain.

[5]Department of Functional Neuroimaging, Service of Nuclear Medicine, CUB Hôpital Erasme, Université libre de Bruxelles (ULB), Brussels, Belgium.

Corresponding author: Brice Marty, Laboratoire de Cartographie fonctionnelle du Cerveau, UNI – ULB Neuroscience Institute, 808 route de Lennik, 1070 Brussels, Belgium. Telephone: +3225556602, Fax: +3225556631, E-mail: bmarty@ulb.ac.be

Abstract

This study investigates whether movement kinematics modulates similarly the rolandic α and β rhythm amplitude during executed and observed goal-directed hand movements. It also assesses if this modulation relates to the corticokinematic coherence (CKC), which is the coupling observed between cortical activity and movement kinematics during such motor actions.

Magnetoencephalography (MEG) signals were recorded from 11 right-handed healthy subjects while they performed or observed an actor performing the same repetitive hand pinching action. Subjects' and actor's forefinger movements were monitored with an accelerometer. Coherence was computed between acceleration signals and the amplitude of α (8–12 Hz) or β (15–25 Hz) oscillations. The coherence was also evaluated between source-projected MEG signals and their β amplitude.

Coherence was mainly observed between acceleration and the amplitude of β oscillations at movement frequency within bilateral primary sensorimotor (SM1) cortex with no difference between executed and observed movements. Cross-correlation between the amplitude of β oscillations at the SM1 cortex and movement acceleration was maximal when acceleration was delayed by ~100 ms, both during movement execution and observation. Coherence between source-projected MEG signals and their β amplitude during movement observation and execution was not significantly different from that during rest.

This study shows that observing others' actions engages in the viewer's brain similar dynamic modulations of SM1 cortex β rhythm as during action execution. Results support the view that different neural mechanisms might account for this modulation and CKC. These two kinematic-related phenomena might help humans to understand *how* observed motor actions are actually performed.

1. Introduction

At rest, the human brain activity usually exhibits an arch-shaped rolandic "mu rhythm", initially described by Gastaut et al. (1952) using scalp electroencephalography (EEG). *This rhythm that appears over sensorimotor regions, is characterized by two main frequency components peaking at ~10 Hz (alpha frequency) and ~20 Hz (beta frequency) that appear to be related to different functional processes.* The alpha component mainly (but not exclusively) reflects somatosensory cortical processes, while the beta component appears predominantly involved in motor-cortex function (Salmelin and Hari, 1994a).

The two mu-rhythm components are transiently suppressed during movements and enhanced for few seconds shortly after movements' offset (Pfurtscheller et al., 1996; Salmelin and Hari 1994a). Interestingly, the mu rhythm is also partly suppressed and thereafter enhanced by tactile stimulation (Salenius et al., 1997; Cheyne et al., 2003; Bauer et al., 2006;), motor preparation (Nagamine et al., 1996; Pfurtscheller and Lopes da Silva, 1999), passive movements (Salmelin and Hari, 1994a; 1994b; Cassim et al., 2001), motor imagery (Schnitzler et al., 1997), and observation of others' motor acts (Hari et al., 1998; Caetano et al., 2007; Kilner et al., 2009; Avanzini et al., 2012). Not surprisingly, the magnitude of the modulation during action execution is higher than that during action observation (Caetano et al., 2007). *The finding that movement execution and observation modulate the mu rhythm in a rather similar manner might be explained by the presence of mirror neurons in the primary motor (M1) cortex (Vigneswaran et al., 2013) or by activation of motor areas in both conditions (Neuper et al., 2006).* Alternatively, activity in M1 cortex during movement observation might be merely modulated through strong reciprocal cortico-cortical connections with premotor areas that are themselves truly activated

during motor execution and observation (for a review, see Kilner and Frith, 2007).

In everyday life, movements seldom appear in isolation but are contiguous and complex. During observation of such complex motions, movement velocity dynamically modulates beta-band MEG amplitude in the primary sensorimotor (SM1) cortex, as shown by a MEG study wherein short video clips of sinusoidal up and down arm movements were presented (Press et al., 2011). Specifically, the beta-band amplitude is at lowest before the point of maximum velocity and at highest before the point of minimum velocity. Similarly, in a high-density EEG study that used video clips of four types of discrete hand motor actions (two of them being cyclic and the others being non-cyclic), the centro-parietal beta-band amplitude was transiently enhanced after each time hand velocity approached zero (Avanzini et al., 2012). Interestingly, an EEG study demonstrated that the speed of both executed and imagined hand actions modulates the mu rhythm, in a way that movement speed can be successfully decoded from the variations in mu rhythm amplitude (Yuan et al., 2010). *Finally, other MEG and EEG studies demonstrated that the alpha and the beta components of the mu rhythm are significantly modulated by movement kinematics during various finger movement tasks such as fingers flexion-extension and finger tapping (Houweling et al., 2010; Seeber et al., 2016; Zhou et al., 2016).* Still, to the best of our knowledge, dynamic modulation of the mu rhythm by movement kinematics has not been compared *per se* during similar motor action execution and observation. Also, the kinematic-related mu modulation has not been demonstrated for ecologically valid goal-directed hand actions.

Here, we explored the influence of movement kinematics on the alpha (8–12 Hz) and the beta (15–25 Hz) components of the mu rhythm during execution and observation of goal-directed hand actions performed in natural experimental

conditions. Goal-directed hand actions were used as they have been shown to induce stronger modulation of rolandic beta rhythm than non-goal directed actions (Jarvelainen et al., 2004). Using MEG recordings and coherence analysis, we searched for the evidence of coupling between movement acceleration and the amplitude of alpha- and beta-band components of the rolandic mu rhythm in both movement conditions. We expected the kinematics of goal-directed hand actions to dynamically modulate mu-rhythm amplitude in a similar fashion during both execution and observation.

Finally, previous studies have demonstrated that activity of a large sensorimotor network is phasically coupled with movement kinematics during both non-goal and goal directed hand movement execution and observation *(i.e., the corticokinematic coherence (CKC), see Schalk et al., 2007; Jerbi et al., 2007; Bourguignon et al. 2011, 2012, 2013; Marty et al. 2015a).* Such phase coupling typically occurs at movement frequency and its first harmonics (i.e., for frequencies lower than those of the mu rhythm), with its main cortical source located at the SM1 cortex contralateral to movement (*Jerbi et al., 2007;* Bourguignon et al., 2011, 2012, 2013; Marty et al. 2015a). Therefore, to obtain further insights into how movement kinematics modulates cortical rhythmic activity, we also evaluated the coupling between source-projected MEG signals (i.e., for CKC) and mu rhythm amplitude.

2. Materials and methods

2.1. Participants

The present study is a reanalysis of two experimental data sets obtained from distinct groups of healthy adult subjects. The first group (Group A; 11 subjects, 5 males, 6 females; mean age 30.8 yrs, range 26–41 yrs) was previously reported in Marty et al. (2015a) and the second group (Group B; 10 subjects, 7 males, 3 females; mean age 31.3 yrs, range 25–41 yrs) was previously reported in Marty et al. (2015b). *Six subjects participated in both studies.*

All participants were right-handed according to the Edinburgh handedness inventory (Oldfield, 1971) and had no prior history of neurological or psychiatric disorder. They participated after written informed consent. The study had prior approval by the ULB-Hôpital Erasme Ethics Committee.

2.2. Experimental paradigm

Subjects from Group A underwent three 5-min experimental conditions (*Self*, *Other*, and *Rest*) while their MEG activity was recorded. These conditions have been described in details in Marty et al. (2015a; 2015b).

Figure 1 illustrates the *Self* and the *Other* conditions.

Briefly, in the *Self* condition, a set of colored foam beads (~60 green, ~30 red, purple, orange or yellow; thickness ~4 mm; area ~1 cm^2) was placed on the MEG table in front of the subjects. They were asked to pinch the green beads with the right hand, and to move them into a pot placed on the right of the beads. The ensuing repetitive movement was operated at ~1 Hz until the cup was full; the whole process being repeated successively during 5 min. The left hand was kept on the left thigh. Subjects were asked to gaze at the center of the beads heap during the hand

movements to minimize eye movements. The subjects' hand actions were monitored with a 3-axis accelerometer (Acc, ADXL335 iMEMS Accelerometer, Analog Devices, Inc., Norwood, MA, USA) attached to the right index finger.

In the *Other* condition, subjects observed an experimenter performing the same task as in *Self*. The experimenter sat in front of the subjects (at 1.5 m) inside the magnetically shielded room (MSR). A screen separated the subjects and the experimenter in a way that all that was left visible to the subjects was the experimenter's right hand, the beads, and the pot. The experimenter's right index finger movements were monitored with an Acc.

During the *Rest* condition, subjects were instructed to relax, not to move, and to gaze at a point on the opposite wall of the MSR.

In the *Self* condition, the subjects saw their hand movements. In order to assess the potential influence of ensuing visual afferences on the results obtained for this condition, we also included a control condition in which subjects from Group B performed self-paced flexion-extensions of the right-hand fingers at ~1 Hz (*Self_nongoal*). This condition was described in details in Marty et al. (2015b). It lasted 11 min and was interrupted by 3 pauses of 1 min. Subjects were asked to fixate a point in the MSR and to not look at their moving hand so as to avoid any gaze contact with their hand during movements. They were also asked to avoid touching the thumb with the other fingers during the flexions in order to minimize tactile input. If present, the dynamic modulation of mu rhythm by movement kinematics in this group of subjects would not support a major role of visual afferences in the kinematic-related modulation of mu rhythm during movement execution. The subjects' hand actions were monitored with an Acc attached to the nail of the right forefinger. Also, a total of ~3-min of *Rest* data per subject were extracted from the

pauses between the periods of finger movements.

In all conditions, subjects wore earplugs to minimize movement-related auditory contamination during movement conditions.

—Place Figure 1 about here—

2.3. Data acquisition

Neuromagnetic cortical activity was recorded with a whole-scalp-covering neuromagnetometer placed in a lightweight MSR (Vectorview & Maxshield™; Elekta Oy, Helsinki, Finland) installed at the CUB Hôpital Erasme (for more details about the MEG system and MSR used, see Carrette et al., 2011; De Tiege et al., 2008). Four head-tracking coils monitored subjects' head position inside the MEG helmet during the MEG recordings. The locations of the coils and at least 150 head-surface (on scalp, nose, and face) points with respect to anatomical fiducials were digitized with an electromagnetic tracker (Fastrak, Polhemus, Colchester, VT, USA). In subjects from Group A only, (1) vertical and horizontal electrooculograms (EOGs) monitored eye movements and blinks, (2) bipolar surface electromyogram (EMGs) were recorded from the first dorsal interosseous (FDI, ~10 mm inter-electrode distance) and extensor digitorum communis (EDC, ~20 mm inter-electrode distance) muscles bilaterally, and (3) electrocardiogram (ECG) was recorded with two electrodes placed below the clavicles. The recording bandpass was 0.1–330 Hz for MEG, EMG, EOG, and ECG, and 0–330 Hz for Acc; all signals being synchronously sampled at 1 kHz. High-resolution 3D-T1 cerebral magnetic resonance images (MRIs) were acquired with a 1.5-T MRI scanner (Intera, Philips, The Netherlands) at the CUB Hôpital Erasme.

2.4. Data preprocessing

Continuous MEG data were first preprocessed off-line using the signal space separation method (Taulu et al., 2005) to suppress external interferences and to correct for head movements. Using a similar approach as in Marty et al. (2015a), independent component analysis (ICA) was then applied to band-passed (1–25 Hz) MEG signals obtained in subjects from Group A, and ~2 components corresponding to eye-blink and heart-beat artifacts were identified in each subject and subsequently subtracted from raw MEG signals. *The band-pass filter used to that effect was designed in the frequency domain with zero-phase and 1-Hz-wide squared-sine transitions from 0 to 1 and 1 to 0 (e.g., the filter rose from 0 at 0.5 Hz to 1 at 1.5 Hz and ebbed from 1 at 24.5 Hz to 0 at 25.5 Hz). The same type of filter was used through the analysis.* The amplitudes of MEG signals in the alpha- (8–12 Hz) and the beta (15–25 Hz) frequency bands were then extracted using the Hilbert transform in both groups of subjects.

The Acc signal was computed at each time sample as the Euclidian norm of the band-passed (0.1–145 Hz) Acc channels.

Finally, signals from alpha- and beta-band amplitude and Acc were split into 3-s epochs with 1.5-s overlap, leading to a frequency resolution of ~0.33 Hz (Bortel and Sovka, 2007). Epochs in which the filtered MEG amplitude exceeded 3 pT (magnetometers) or 0.7 pT/cm (gradiometers) were marked as artifact-contaminated and excluded from further analysis.

2.5. Coherence analyses between accelerometer and brain signals in sensor space

For each movement condition (*Self, Other, Self_nongoal*), the synchronization of Acc amplitude signals with alpha-band *(Coh_{α})* and beta-band *(Coh_{β})* amplitudes

was separately assessed using coherence analysis in sensor space (Halliday et al., 1995). Coherence analysis is an extension of Pearson correlation coefficient to the frequency domain, which determines the degree of coupling between two signals, providing a number between 0 (no linear dependency) and 1 (perfect linear dependency) for each frequency (Halliday et al., 1995). *In particular, Coh_{α} and Coh_{β} quantified the coupling between amplitude modulation of alpha- and beta-band power at each sensor separately and the kinematics of—executed or observed—movements.*

For each movement condition (Self, Other, Self_nongoal) and component of the mu rhythm (alpha and beta), the frequencies that showed significant sensor-space coherence were identified and defined as "peak coherence frequencies" for subsequent source-level coherence analyses.

2.6. Source-level coherence analyses

Coherence analysis was performed in source space to identify the cortical sources of significant Coh_{α} and Coh_{β}. To this end, the following steps adapted from Marty et al. (2015a) were used: (1) MRIs segmentation (Freesurfer software; Martinos Center for Biomedical Imaging, Massachusetts, USA), (2) MEG-MRI coregisteration using fiducials and head-surface points, (3) MEG forward modeling on a homogeneous 5-mm-grid source space covering the whole brain (MNE suite; Martinos Center for Biomedical Imaging, Massachusetts, USA) with current dipoles orientations constrained to the plane tangential to the skull, (4) source-space projection using a minimum-variance beamformer (Van Veen et al., 1997) based on both planar gradiometers and magnetometers divided by their noise variance (estimated from the continuous *Rest* MEG data), (5) computation of coherence maps between source-level alpha- and beta-band amplitudes and Acc amplitude signals for

each movement condition (*Self, Other, Self_nongoal*) and peak coherence frequency, and (6), for the sake of statistical testing, computation of *Rest* coherence maps of source-level alpha- and beta-band amplitudes at *Rest* with the Acc amplitude signal from each movement condition (*Self, Other, Self_nongoal*).

We finally attempted to uncover the link between the coupling of Acc signals with alpha/beta rhythm amplitude and that of Acc and source signals (i.e., the CKC) as reported in Marty et al. (2015a*). To that aim, for each condition (Self, Other and Rest) and each source, we evaluated the coherence between source signal and source alpha/beta amplitude at the peak coherence frequencies. In other words, we used coherence to quantify the "phase–amplitude" coupling in the source-space, with frequencies for phase set to the peak coherence frequencies, and frequencies for amplitude set to alpha (8–12 Hz) and beta (15–25 Hz) frequencies.*

2.7. Group-level analyses in source space

Individual coherence maps were then combined into a group-level coherence maps. For that purpose, we first estimated a non-linear transformation from individual MRIs to the standard Montreal Neurological Institute (MNI) brain computed using the spatial normalization algorithm implemented in Statistical Parametric Mapping (SPM8, Wellcome Trust Centre for Neuroimaging, London, UK). This transformation was then applied to individual MRIs and each coherence map. This operation resulted in a coherence map normalized in the MNI space for each subject, movement condition (*Self, Other, Self_nongoal*), component of the mu rhythm (alpha and beta), and peak coherence frequency. Coherence maps at the group level were then produced using a generalized averaging procedure consisting in computing the group mean of the Fisher z-transform of the square root coherence, and applying the inverse

Fisher z-transform to the result. This procedure yields an unbiased estimation of mean coherence at the group level (Rosenberg et al., 1989). In practice, this method also lessens the relative contribution of subjects characterized by high coherence values (Bourguignon et al., 2012). A similar procedure was applied to coherence maps computed between source signals and their alpha/beta amplitude at the peak coherence frequencies.

2.8. Cross-correlation between acceleration and MEG alpha- and beta-band amplitude

We used a cross-correlation analysis to better characterize the causal relationship between hand acceleration and MEG alpha- and beta-band amplitude fluctuations in *Self* and *Other*. The cross-correlation was evaluated between log-transformed Acc amplitude and alpha- or beta-band amplitude of sources displaying significant (see 2.9.3.) local maxima of Coh_{α} or Coh_{β}. This analysis was performed directly at the group level, with data from individual subjects temporally concatenated. Individual subjects' data were standardized and time was normalized by individual mean duration of a movement cycle (*i.e.,* 1/F0 with F0 the frequency of movement cycles) prior to concatenation.

2.9. Statistical analyses

2.9.1. Coherence at the sensor level

For each movement condition (Self, Other, Self_nongoal) and component of the mu rhythm (alpha and beta), the statistical significance of individual coherence levels was assessed with surrogate-data-based statistics, which intrinsically corrects for multiple-comparisons and takes into account the temporal autocorrelation within

signals. Specifically, a significance threshold was computed for the maximum coherence across all gradiometers and across 0.33–5.0 Hz. For each subject, 1000 surrogate coherence spectra were obtained by computing Coh_{α} or Coh_{β} based on original MEG signals and Fourier transform surrogates of the Acc signals; the Fourier transform surrogate preserving the power spectrum while replacing the phase of Fourier coefficients by random angles (Faes et al., 2004). Then, a single maximum coherence value across all gradiometers and frequencies in the 0.33–5.0 Hz range was extracted for each surrogate coherence spectrum. The 95th percentile of this maximum statistic yielded the significance threshold for the coherence at $p < 0.05$ corrected for multiple comparisons (channels and frequencies).

2.9.2. Statistical differences in movement frequency and coherence level

The effect of condition and peak coherence frequency on sensor-level coherence and movement frequency between conditions were tested with the Friedman test (non-parametric repeated-measures 1-way ANOVA). The threshold for statistical significance was set to $p < 0.05$.

2.9.3. Coherence at the source level

Statistical significance of the local coherence maxima identified in group-level coherence maps, against values obtained from the associated Rest coherence maps, was assessed with a non-parametric permutation test that intrinsically corrects for multiple spatial comparisons (Nichols and Holmes, 2002), *following the procedure described in* Bourguignon et al. (2012).

In practice, group-level difference maps were obtained by subtracting Fisher z-transformed *Self, Other*, and *Self_nongoal* with the corresponding *Rest* group-level

coherence maps. Under the null hypothesis that coherence maps are identical in all experimental conditions, the labels *Self, Other,* or *Self_nongoal* and *Rest* are exchangeable prior to difference maps computation (Nichols and Holmes, 2002). To reject this hypothesis and compute a threshold of statistical significance for the correctly labeled difference map, the sample distribution of the maximum of the difference map's absolute value was obtained from the exhaustive permutation set (i.e., 2048 permutations). *The threshold at $p < 0.05$ intrinsically corrected for the multiple spatial comparisons was computed as the 95^{th} percentile of the sample distribution* (Nichols and Holmes, 2002). All suprathreshold local coherence maxima were then interpreted as indicative of brain regions showing statistically significant coherence with the kinematics of the executed or the observed hand movements.

We applied the same method to the coherence maps computed between source signals and their alpha/beta amplitude at the peak coherence frequencies to disclose couplings significantly higher in movement conditions (*Self* or *Other*) compared to *Rest*. We also tested the null hypothesis that coherence maps are identical regardless of the movement condition (*Self* and *Other*) using a similar approach.

The above described permutation tests based on a maximum statistic may be too conservative (type II error) for voxels other than those with high coherence level (Nichols and Holmes, 2002). Therefore, permutation tests were repeated within regions of interest (ROIs, 3-cm-radius sphere centered on MNI coordinates taken from the literature) for local coherence maxima located in an anatomical region belonging to the SM1 cortices that did not reach significance using a methodology previously described (Bourguignon et al., 2012). The rationale guiding this additional ROI-based analysis was to avoid type II errors due to the statistical method used.

2.9.4. Cross-correlation between accelerometer and MEG alpha- and beta-band amplitudes

The statistical significance of the cross-correlation of Acc with alpha- and beta-band amplitudes was assessed similarly to sensor-level coherence. Briefly, 1000 surrogate correlation traces were obtained by computing the cross-correlation between log-transformed Fourier-transform-surrogate Acc amplitude signals and alpha-/beta-band source(s) amplitude. The distribution of the maximal correlation value across all brain voxels and time delays between –1/F0 and +1/F0 was assessed, and its 95^{th} percentile yielded the significance threshold at corrected $p < 0.05$.

3. Results

3.1. Coherence analyses at the sensor level

The mean ± standard deviation (SD) movement rate (F0), including the picking and placing of an item, was 1.00 ± 0.15 Hz for *Self* and 0.79 ± 0.22 Hz for *Other*. We have previously reported a trend towards a difference in movement frequency between the conditions (p = 0.057) and no evidence of rhythmic movement of the subjects' upper limbs synchronized with the experimenter's movements during *Other* (Marty et al., 2015a). In *Self_nongoal,* F0 was 1.10 ± 0.20 Hz, which was not significantly different from that in *Self* and *Other* (p = 0.87).

Coh_α peaked at F0 over posterior MEG sensors and was significant in 5 out of 11 subjects during *Self* (mean ± SD coherence level 0.10 ± 0.05) and in 4 subjects during *Other* (0.08 ± 0.03); these levels did not differ between *Self* and *Other* (p = 0.22*). Coh_β peaked at F0 over posterior and central MEG sensors, and* was significant in 8 subjects during *Self* (0.14 ± 0.1) and in 6 subjects during *Other* (0.10 ± 0.06); with no difference between *Self* and *Other* (p = 0.31). During *Self_nongoal,* significant *Coh_α* occurred at F0 in 2 out of 10 subjects (0.14 ± 0.04) and Coh_β peaked at F0 over left central MEG sensors and was significant in 6 subjects (0.28 ± 0.20). No significant coherence was observed at harmonics of movement frequency in any of the conditions.

Based on these data, we only considered F0 as peak coherence frequency for subsequent source-level analyses.

3.2. Coherence analyses at the source level

Coherence analysis was performed in source space at F0 to identify the neuronal networks underlying the coherence observed in sensor space.

Coh$_\alpha$ was significant in the left striate and extrastriate visual cortices in *Self* ($p <$ 0.05), and was not significant in *Other* and *Self_nongoal* (*ps* > 0.05). No local coherence maximum was observed in the SM1 cortex in any of the conditions, even at more liberal thresholds.

Figure 2 illustrates the source locations of significant Coh$_\beta$ *at F0 at the group level and Figure 3 at the subject level*. At the group level, in *Self*, coherent sources were located at the right SM1 hand area (SM1$_{ha}$, MNI coordinates [49 –25 58] mm, group coherence 0.05) and the visual areas of the right hemisphere. In addition, a clearly distinct, although weaker, local coherence maximum was found in the left SM1$_{ha}$ ([–49 –17 60] mm, group coherence 0.03, ROI-based p = 0.031). At the individual level, *local coherence maxima were observed at the left SM1 cortex in 7 subjects and at the right SM1 cortex in 6 subjects*. In *Other*, the source locations were rather similar. Significant coherence was found at the group level in the bilateral SM1$_{ha}$ (left SM1$_{ha}$, [–38 –36 64] mm, group coherence 0.04; right SM1$_{ha}$, [44 –28 51] mm, group coherence: 0.03) as well as in visual areas. *Local coherence maxima were observed at the left or the right SM1 cortices in 5 subjects*. In addition, we did not find any significant difference between *Self* and *Other Coh*$_\beta$ maps. During *Self_nongoal,* significant coherence was only found at the left SM1$_{ha}$ ([–34 –12 60] mm, group coherence: 0.17).

Figure 2 (bottom, right) also illustrates the conjunction map of significant *Coh*$_\beta$ during both *Self* and *Other*. Voxels of the conjunction map are set to 1 if they correspond to significant *Coh*$_\beta$ during both *Self* and *Other*, and to 0 otherwise. This conjunction map demonstrates that the beta-band amplitude within bilateral SM1$_{ha}$ and visual areas exhibit coupling with movement kinematics regardless of the execution or observation role of the subjects.

—Place Figures 2 and 3 about here—

To obtain more insight into the temporal dynamic of beta-band amplitude with bilateral $SM1_{ha}$, we computed its cross-correlation with Acc amplitude signals. Figure 4 shows that beta-band amplitude was positively correlated with Acc amplitude approximately one tenth of movement cycle (~100 ms) later in both conditions and both hemispheres (*Self*–left: delay in 1/F0 units = 0.12, $r = 0.02$, $p = 0.002$; *Self*–right: delay = 0.12, $r = 0.035$, $p < 0.001$; *Other*–left: delay = 0.15, $r = 0.042$, $p < 0.001$; *Other*–right: delay = 0.06, $r = 0.016$, $p = 0.058$). Such a delay is best seen when beta-band amplitude is averaged time-locked to Acc amplitude peaks (see Fig. 4).

—Place Figure 4 about here—

These results demonstrate that beta-band amplitude is significantly coupled with movement kinematics at F0. Interestingly, a previous study based on the same MEG data set demonstrated that source-projected MEG time series are also phasically coupled with movement kinematics at F0 (i.e., the CKC, see Marty et al., 2015a). We therefore searched for the existence of coherence between source-projected MEG signals and their beta-band amplitude at F0 ("phase–amplitude" coupling) during *Self* and *Other* compared *with Rest*. In *Self*, the phase–amplitude coupling peaked at bilateral sensorimotor cortices but associated values did not reach statistical significance (left SM1 ROI, $p = 0.17$; right SM1 ROI, $p = 0.12$). In *Other*, maps of phase–amplitude coupling were not suggestive of any peak at SM1 cortices (left SM1 ROI, $p = 0.51$; right SM1 ROI, $p = 0.93$).

4. Discussion

We found that observing others' goal-directed hand actions engages similar kinematic-related modulation of the beta (15–25 Hz) frequencies of bilateral SM1 cortices in the viewer's brain as during own hand actions. This dynamic modulation was characterized by a positive correlation between SM1 cortex beta-band amplitude and finger movement acceleration amplitude that was maximal when acceleration amplitude was delayed by ~100 ms during both executed and observed motor actions. Also and importantly, we did not find any evidence supporting a link between this dynamic modulation of the beta-band mu rhythm amplitude and CKC.

We found that movement kinematics phasically modulates bilaterally SM1 beta rhythm amplitude during execution of goal-directed hand actions. This finding is in line with previous observations showing that movement velocity can be decoded based on the variations in mu-rhythm amplitude during movements (Yuan et al., 2010), and that the SM1-cortex mu rhythm is modulated by movement kinematics during various types of finger movements (*Houweling et al., 2010; Seeber et al., 2016;* Zhou et al., 2016). In the present study, we found a positive correlation between acceleration and beta-band amplitudes during movement execution at bilateral SM1 cortices. This correlation was maximum when a delay of ~100 ms was added to acceleration amplitude signals, which indicates a causal effect of acceleration changes on subsequent modulations of SM1 cortex beta-band amplitude. *This finding is difficult to compare with those of previous studies because of differences in experimental tasks: we used non-sinusoidal goal directed hand movements and acceleration amplitude as kinematic signal while previous studies used sinusoidal non-goal directed hand movements and amplitude or position as kinematic signals. In addition, we used Euclidian norm of the 3 axis Acc signals,*

which makes the comparison even more delicate (Houweling et al., 2010; Seeber et al., 2016; Zhou et al., 2016). Still, this finding complements previous studies by showing that movement kinematics indeed dynamically modulates bilateral SM1 cortex beta-band power during goal directed hand movements. Also, during goal-directed movement execution, the bilateral modulation of SM1 beta rhythm amplitude by movement acceleration rather predominated over the SM1 cortex ipsilateral to the moving fingers. This finding is in agreement with those of Seeber et al. (2016) but not with those of Zhou et al. (2016) nor with our data obtained with a non-goal directed hand action. Further studies on brain responses to different movement types in the same subjects would be needed to clarify the hemispheric dominance of this kinematic-related beta rhythm amplitude modulation.

When executing movements, subjects were seeing their own hand during action execution, which likely explains the occurrence of Coh_{β} also in occipital areas. One could therefore argue for a potential influence of visual input on the modulation of the rolandic mu rhythm by movement kinematics. To rule out this possibility, we used, as control condition, data recorded in another set of subjects who made self-paced flexion–extension movements of the right-hand fingers at ~1 Hz without looking at their moving hand. In this dataset, we found similar amplitude modulation of the mu rhythm at the SM1 cortex contralateral to hand movement. Although obtained in a non-goal directed task and in another group of subjects, these results suggest that visual inputs play only a minor role in the observed modulation of SM1 cortex mu rhythm amplitude during executed movements and that this modulation is mainly driven by movement kinematics *per se*.

We found similar phasic modulation of beta-band amplitude in bilateral SM1 cortices when subjects executed and observed motor actions. This modulation

identified during movement observation cannot be ascribed to subtle movements that would be performed by the subjects during action observation. Indeed, we previously found no evidence of coupling between subjects' upper limb movements and the experimenter's movements (Marty et al., 2015a). Therefore, beta-band amplitude modulation during movement observation should be driven by the observed movement kinematics. Interestingly, time-delays between Acc and SM1 cortex beta-band amplitudes were similar (~100 ms) during action execution and observation. Previous studies focused on the dynamic modulation of rolandic beta-band amplitude by movement velocity during observation of simple sinusoidal or discrete movements (Avanzini et al., 2012; Lippi et al., 2012; Press et al., 2011). In contrast, we used non-sinusoidal repetitive movements and monitored movement kinematics with an Acc. A direct comparison with their results is therefore not straightforward. Still, our data bring further evidence that observed movement kinematics modulates the amplitude of rolandic beta-band rhythm. Specifically, our results demonstrate that beta-band amplitude is coupled with movement kinematics not only for sinusoidal or discrete movements as previously reported (Press et al., 2011; Avanzini et al. ,2012), but also for continuous and repetitive goal-directed movements during both movement observation and execution.

We have previously shown the existence of another coupling phenomenon between SM1 cortex signals and movement kinematics, which we termed the CKC (Bourguignon et al., 2011). Like the mu rhythm modulation we here report, CKC is seen during executed and observed—goal and non-goal directed—repetitive movements (Bourguignon et al., 2012, 2013; Piitulainen et al., 2013a; Marty et al., 2015a). *Previous studies have demonstrated that, during movement execution, the CKC phenomenon mainly reflects movement-related somatosensory proprioceptive*

afferent input to the contralateral SM1 cortex Bourguignon et al., 2015; Piitulainen et al., 2013b. The observation of similar CKC during movement observation suggested that this phasic "mirroring" possibly driven by visual analysis of observed movement kinematics might help observers understand the somatosensory (i.e., proprioceptive) consequences of others' motor actions (for a review, see, e.g., Keyser et al. Nat Rev Neurosci 2010). Interestingly, in the present study, the coupling between source signals and their beta-band amplitude at movement frequency was not significantly increased during movement execution and observation compared with rest. This finding suggests that the interplay between the mu rhythm and slower (~1 Hz) brain fluctuations is not specific of sensorimotor processes. *Also, it might suggest that the kinematic-related beta-band power modulation at bilateral SM1 cortices may represent the processing of movement kinematics itself. Indeed, some experimental evidence suggests that movement-related reduction in beta-band power is directly related to the disinhibition of neuronal populations involved in the computations of movement parameters (Brinkman et al., 2014). Studies comparing active with passive finger movements will be of utmost interest to address this issue.*

Finally, the present results are suggestive of the existence of key differences between the mirroring phenomenon observed in human and monkeys. Indeed, in monkeys, the mirror system seems to mainly encode the goal of the observed motor acts and not the kinematic features of an observed action (for reviews, see e.g., Rizzolatti and Craighero, 2004 and Rizzolatti and Sinigaglia, 2010). *Contrastingly, the present and previous MEG/EEG studies suggest that human SM1 cortex is sensitive to some aspects of movement kinematics during action observation*. Further dedicated studies should be performed to properly address that critical issue.

In conclusion, we have demonstrated that beta-band amplitude at

bilateral SM1 cortex is modulated by the kinematics of repetitive goal-directed hand movements, in a similar manner during movement execution and observation. This finding suggests that action observation engages, in the viewer's brain, similar neural kinematic-related mechanisms to those involved in the execution of the same hand actions. Also, results support the view that different neural mechanisms might account for this modulation and CKC. *These two phasic mirroring phenomena might represent a prerequisite for the human brain to understand how observed actions are actually performed.*

5. Acknowledgments

The authors declare that they have no conflict of interest.

Xavier De Tiège is Postdoctorate Clinical Master Specialist at the Fonds de la Recherche Scientifique (FRS-FNRS, Brussels, Belgium). This work was supported by the program Attract of Innoviris (Grant 2015-BB2B-10 to Mathieu Bourguignon), the Spanish Ministry of Economy and Competitiveness (grant PSI2016-77175-P to Mathieu Bourguignon), the Marie Skłodowska-Curie Action of the European Commission (grant #743562 to Mathieu Bourguignon), a **"**Brains Back to Brussels**"** grant to Veikko Jousmäki from the Institut d'Encouragement de la Recherche Scientifique et de l'Innovation de Bruxelles (Brussels, Belgium), European Research Council (Advanced Grant #232946 to Riitta Hari), the Fonds de la Recherche Scientifique (FRS-FNRS, Belgium, Research Credits: J009713), and the Academy of Finland (grants #131483 and #263800). The MEG project at the ULB-Hôpital Erasme (Brussels, Belgium) is financially supported by the Fonds Erasme.

We thank Helge Kainulainen and Ronny Schreiber at the Brain Research Unit (Aalto University, Finland) for technical support. We also thank Professor Stéphane Swillens at the Université libre de Bruxelles (ULB), Professor Riitta Hari (Aalto University) and Doctor Stéphanie Grégoire (Mc Gill University) for their support and advices.

6. References

Avanzini, P., Fabbri-Destro, M., Dalla Volta, R., Daprati, E., Rizzolatti, G., Cantalupo, G., 2012. The dynamics of sensorimotor cortical oscillations during the observation of hand movements: an EEG study. PLoS One 7, e37534.

Bauer, M., Oostenveld, R., Peeters, M., Fries, P., 2006. Tactile spatial attention enhances gamma-band activity in somatosensory cortex and reduces low-frequency activity in parieto-occipital areas. J Neurosci 26, 490-501.

Bortel, R., Sovka, P., 2007. Approximation of statistical distribution of magnitude squared coherence estimated with segment overlapping. Signal Processing 87, 1100-1117.

Bourguignon, M., De Tiège, X., de Beeck, M.O., Pirotte, B., Van Bogaert, P., Goldman, S., Hari, R., Jousmäki, V., 2011. Functional motor-cortex mapping using corticokinematic coherence. Neuroimage 55, 1475-1479.

Bourguignon, M., De Tiege, X., de Beeck, M.O., Van Bogaert, P., Goldman, S., Jousmaki, V., Hari, R., 2012. Primary motor cortex and cerebellum are coupled with the kinematics of observed hand movements. Neuroimage 66, 500-507.

Bourguignon, M., Piitulainen, H., De Tiege, X., Jousmaki, V., Hari, R., 2015. Corticokinematic coherence mainly reflects movement-induced proprioceptive feedback. Neuroimage 106, 382-390.

Brinkman, L., Stolk, A., Dijkerman, H.C., de Lange, F.P., Toni, I., 2014. Distinct roles for alpha- and beta-band oscillations during mental simulation of goal-directed actions. J Neurosci 34, 14783-14792.

Caetano, G., Jousmaki, V., Hari, R., 2007. Actor's and observer's primary motor cortices stabilize similarly after seen or heard motor actions. Proc Natl Acad Sci U S A 104, 9058-9062.

Carrette, E., De Tiege, X., Op De Beeck, M., De Herdt, V., Meurs, A., Legros, B., Raedt, R., Deblaere, K., Van Roost, D., Bourguignon, M., Goldman, S., Boon, P., Van Bogaert, P., Vonck, K., 2011. Magnetoencephalography in epilepsy patients carrying a vagus nerve stimulator. Epilepsy Res 93, 44-52.

Cassim, F., Monaca, C., Szurhaj, W., Bourriez, J.L., Defebvre, L., Derambure, P., Guieu, J.D., 2001. Does post-movement beta synchronization reflect an idling motor cortex? Neuroreport 12, 3859-3863.

Cheyne, D., Gaetz, W., Garnero, L., Lachaux, J.P., Ducorps, A., Schwartz, D., Varela, F.J., 2003. Neuromagnetic imaging of cortical oscillations accompanying tactile stimulation. Brain Res Cogn Brain Res 17, 599-611.

De Tiege, X., de Beeck, M.O., Funke, M., Legros, B., Parkkonen, L., Goldman, S., Van Bogaert, P., 2008. Recording epileptic activity with MEG in a light-weight magnetic shield.

Faes, L., Pinna, G.D., Porta, A., Maestri, R., Nollo, G., 2004. Surrogate data analysis for assessing the significance of the coherence function. IEEE Trans Biomed Eng 51, 1156-1166.

Gastaut, H., 1952. [Electrocorticographic study of the reactivity of rolandic rhythm]. Rev Neurol (Paris) 87, 176-182.

Halliday, D.M., Rosenberg, J.R., Amjad, A.M., Breeze, P., Conway, B.A., Farmer, S.F., 1995. A framework for the analysis of mixed time series/point process data--theory and application to the study of physiological tremor, single motor unit discharges and electromyograms. Prog Biophys Mol Biol 64, 237-278.

Hari, R., Forss, N., Avikainen, S., Kirveskari, E., Salenius, S., Rizzolatti, G., 1998. Activation of human primary motor cortex during action observation: a neuromagnetic study. Proc Natl Acad Sci U S A 95, 15061-15065.

Houweling, S., Beek, P.J., Daffertshofer, A., 2010. Spectral changes of interhemispheric crosstalk during movement instabilities. Cereb Cortex 20, 2605-2613.

Jarvelainen, J., Schurmann, M., Hari, R., 2004. Activation of the human primary motor cortex during observation of tool use. Neuroimage 23, 187-192.

Jerbi, K., Lachaux, J.P., N'Diaye, K., Pantazis, D., Leahy, R.M., Garnero, L., Baillet, S., 2007. Coherent neural representation of hand speed in humans revealed by MEG imaging. Proc Natl Acad Sci U S A 104, 7676-7681.

Kilner, J.M., Frith, C.D., 2007. A possible role for primary motor cortex during action observation. Proc Natl Acad Sci U S A 104, 8683-8684.

Kilner, J.M., Marchant, J.L., Frith, C.D., 2009. Relationship between activity in human primary motor cortex during action observation and the mirror neuron system. PLoS One 4, e4925.

Lippi, G., Fontana, R., Avanzini, P., Aloe, R., Ippolito, L., Sandei, F., Favaloro, E.J., 2012. Influence of mechanical trauma of blood and hemolysis on PFA-100 testing. Blood Coagul Fibrinolysis 23, 82-86.

Marty, B., Bourguignon, M., Jousmaki, V., Wens, V., Op de Beeck, M., Van Bogaert, P., Goldman, S., Hari, R., De Tiege, X., 2015a. Cortical kinematic processing of executed and observed goal-directed hand actions. Neuroimage 119, 221-228.

Marty, B., Bourguignon, M., Op de Beeck, M., Wens, V., Goldman, S., Van Bogaert, P., Jousmaki, V., De Tiege, X., 2015b. Effect of movement rate on corticokinematic coherence. Neurophysiol Clin.

Nagamine, T., Kajola, M., Salmelin, R., Shibasaki, H., Hari, R., 1996. Movement-related slow cortical magnetic fields and changes of spontaneous MEG- and EEG-brain rhythms. Electroencephalogr Clin Neurophysiol 99, 274-286.

Neuper, C., Wortz, M., Pfurtscheller, G., 2006. ERD/ERS patterns reflecting sensorimotor activation and deactivation. Prog Brain Res 159, 211-222.

Nichols, T.E., Holmes, A.P., 2002. Nonparametric permutation tests for functional neuroimaging: a primer with examples. Hum Brain Mapp 15, 1-25.

Oldfield, R.C., 1971. The assessment and analysis of handedness: the Edinburgh inventory. Neuropsychologia 9, 97-113.

Pfurtscheller, G., Lopes da Silva, F.H., 1999. Event-related EEG/MEG synchronization and desynchronization: basic principles. Clin Neurophysiol 110, 1842-1857.

Pfurtscheller, G., Stancak, A., Jr., Neuper, C., 1996. Post-movement beta synchronization. A correlate of an idling motor area? Electroencephalogr Clin Neurophysiol 98, 281-293.

Piitulainen, H., Bourguignon, M., De Tiege, X., Hari, R., Jousmaki, V., 2013a. Coherence between magnetoencephalography and hand-action-related acceleration, force, pressure, and electromyogram. Neuroimage 72, 83-90.

Piitulainen, H., Bourguignon, M., De Tiège, X., Hari, R., Jousmäki, V., 2013b. Corticokinematic coherence during active and passive finger movements. Neuroscience.

Press, C., Cook, J., Blakemore, S.J., Kilner, J., 2011. Dynamic modulation of human motor activity when observing actions. J Neurosci 31, 2792-2800.

Rizzolatti, G., Craighero, L., 2004. The mirror-neuron system. Annu Rev Neurosci 27, 169-192.

Rizzolatti, G., Sinigaglia, C., 2010. The functional role of the parieto-frontal mirror circuit: interpretations and misinterpretations. Nat Rev Neurosci 11, 264-274.

Rosenberg, J.R., Amjad, A.M., Breeze, P., Brillinger, D.R., Halliday, D.M., 1989. The Fourier approach to the identification of functional coupling between neuronal spike trains. Prog Biophys Mol Biol 53, 1-31.

Salenius, S., Schnitzler, A., Salmelin, R., Jousmaki, V., Hari, R., 1997. Modulation of human cortical rolandic rhythms during natural sensorimotor tasks. Neuroimage 5, 221-228.

Salmelin, R., Hari, R., 1994a. Characterization of spontaneous MEG rhythms in healthy adults. Electroencephalogr Clin Neurophysiol 91, 237-248.

Salmelin, R., Hari, R., 1994b. Spatiotemporal characteristics of sensorimotor neuromagnetic rhythms related to thumb movement. Neuroscience 60, 537-550.

Schalk, G., Kubanek, J., Miller, K.J., Anderson, N.R., Leuthardt, E.C., Ojemann, J.G., Limbrick, D., Moran, D., Gerhardt, L.A., Wolpaw, J.R., 2007. Decoding two-dimensional movement trajectories using electrocorticographic signals in humans. J Neural Eng 4, 264-275.

Schnitzler, A., Salenius, S., Salmelin, R., Jousmaki, V., Hari, R., 1997. Involvement of primary motor cortex in motor imagery: a neuromagnetic study. Neuroimage 6, 201-208.

Seeber, M., Scherer, R., Muller-Putz, G.R., 2016. EEG Oscillations Are Modulated in Different Behavior-Related Networks during Rhythmic Finger Movements. J Neurosci 36, 11671-11681.

Taulu, S., Simola, J., Kajola, M., 2005. Applications of the Signal Space Separation Method. Signal Processiong, IEEE transactions on 53, 3359-3372.

Van Veen, B.D., van Drongelen, W., Yuchtman, M., Suzuki, A., 1997. Localization of brain electrical activity via linearly constrained minimum variance spatial filtering. IEEE Trans Biomed Eng 44, 867-880.

Vigneswaran, G., Philipp, R., Lemon, R.N., Kraskov, A., 2013. M1 corticospinal mirror neurons and their role in movement suppression during action observation. Curr Biol 23, 236-243.

Yuan, H., Perdoni, C., He, B., 2010. Relationship between speed and EEG activity during imagined and executed hand movements. J Neural Eng 7, 26001.

Zhou, G., Bourguignon, M., Parkkonen, L., Hari, R., 2016. Neural signatures of hand kinematics in leaders vs. followers: A dual-MEG study. Neuroimage 125, 731-738.

7. Legend of the figures

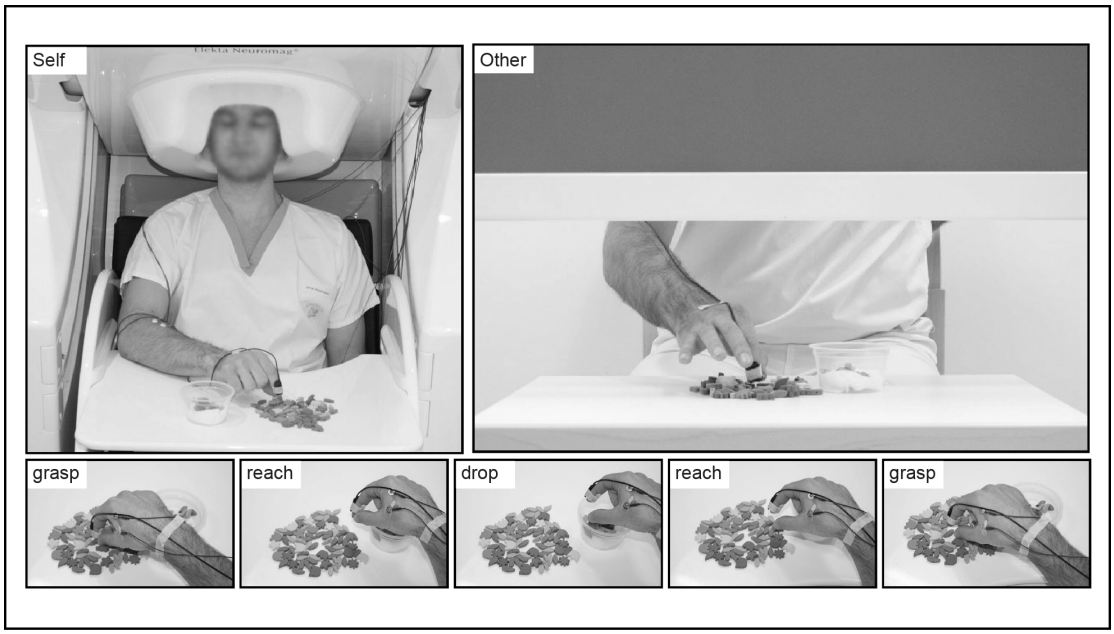

Figure 1

Experimental paradigm. **Top, left**: *Self* condition. Subjects' MEG activity is recorded while they pinch green beads, and move them into a plastic pot placed on the right of the beads heap. **Top, right**: *Other* condition from subjects' point of view. The experimenter executes the same repetitive movements of the *Self* condition. **Bottom**: One movement cycle (grasp, reach, drop, reach, and grasp), identical in the *Self* and *Other* conditions.

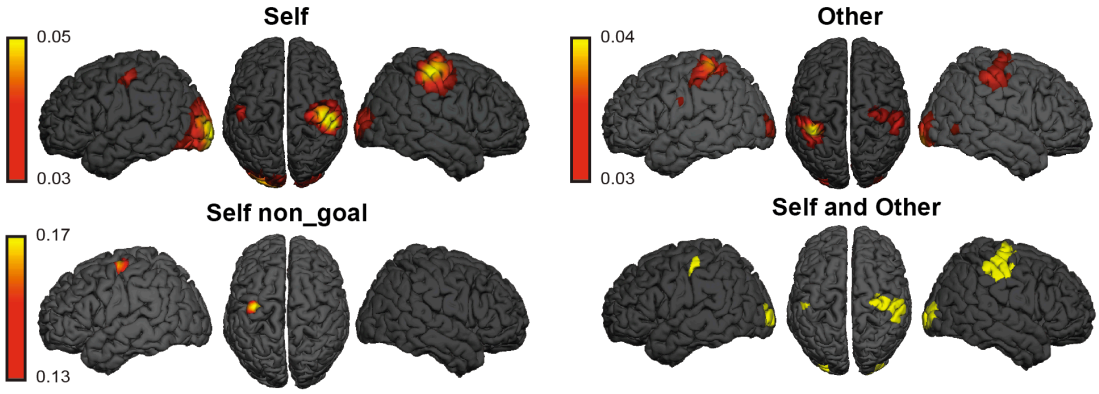

Figure 2

Group-level maps of coherence between hand acceleration amplitude and beta-band amplitude of source-reconstructed signals. The MNI brain is viewed from left, top, and right **Top, Left:** surface rendering of group-level coherence maps during *Self* at movement frequency. Apart from visual areas, coherence peaked in SM1 hand area bilaterally. Maps are thresholded so as to highlight the statistically significant local maximum of coherence in the left SM1 hand area (ROI-based statistics). **Top, Right:** similar maps obtained for *Other*. **Bottom, left**: similar maps obtained for *Self_nongoal*. **Bottom, right:** Brain areas showing significant coupling in both *Self* and *Other.*

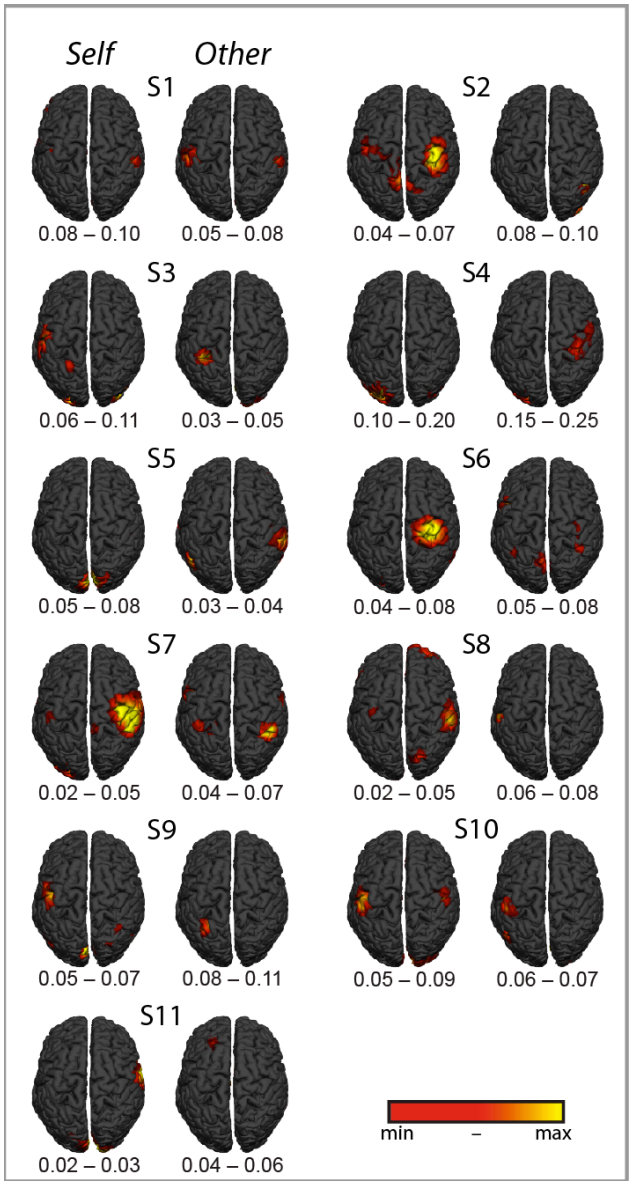

Figure 3

*Subject-level maps of coherence between hand acceleration amplitude and beta-band amplitude of source-reconstructed signals. For each subject, coupling in Self (**Left**) and Other (**Right**) is displayed on the MNI brain viewed from the top. Coherence maps are thresholded at arbitrary coherence values (indicated at the bottom of each brain) to highlight local coherence maxima. For indicative purposes, displayed source-space values can be compared to the significance threshold for individual sensor-space coherence values: 0.09 ± 0.01 (mean ± SD across subjects and conditions).*

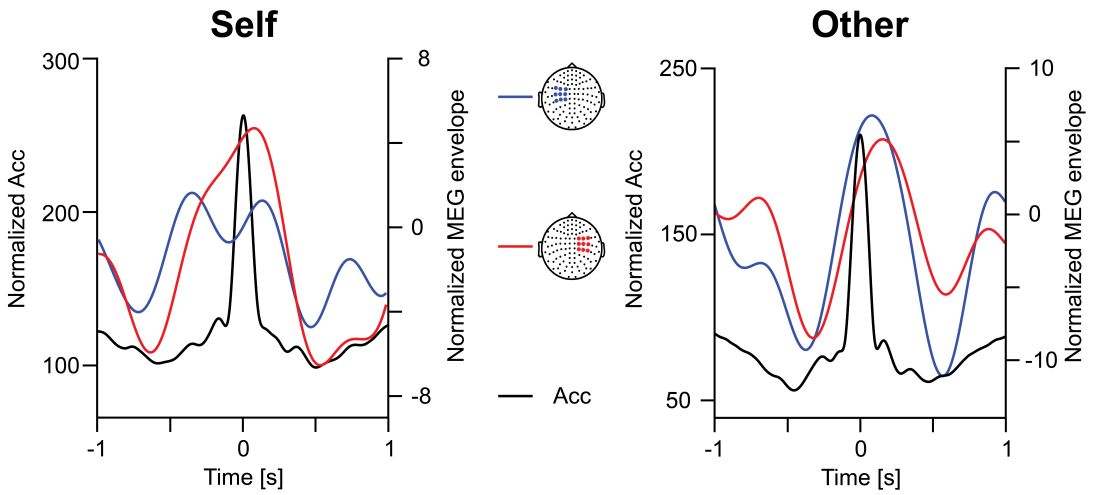

Figure 4

Rolandic beta-band amplitude modulation by movement acceleration amplitude in *Self* (left) and *Other* (right) conditions. Mean acceleration amplitude (black lines) and beta-band amplitude in the left rolandic area (blue lines) and the right rolandic area (red lines) were obtained by averaging 2-s epochs centered on the peaks of acceleration amplitude. The MEG amplitude data were averaged across rolandic sensors (left: blue dots, right: red dots) and normalized by their standard deviation.